

## X-RAY ANALYSIS OF THE ULTRAFINE-GRAINED VT6 TITANIUM ALLOY SUBJECTED TO FLAT ROLLING

V. D. Sitdikov,<sup>1</sup> I. V. Alexandrov,<sup>1</sup> V. N. Danilenko,<sup>2</sup> and V. A. Popov<sup>2</sup>

UDC 539.261

*Results are presented of experimental x-ray diffraction analysis of the microstructure of VT6 titanium alloy billets in ultrafine-grained (UFG) state subjected to flat rolling. The UFG state was formed by six cycles of isothermal multiaxial forging at 650 °C. The regularities of changes of the structural parameters (the lattice parameter, coherently scattering domain size, and microdistortions of the crystal lattice) are revealed depending on the degree of flat rolling reduction.*

**Keywords:** X-ray diffraction analysis, VT6 titanium alloy, UFG structure, isothermal multiaxial forging, flat cross rolling.

### INTRODUCTION

By the present time, the methods of severe plastic deformation (SPD) such as equal-channel angular pressing (ECAP), high-pressure torsion (HPT), and isothermal multiaxial forging (MAF) have actively been developed [1–3]. These methods allow bulk nanostructured and ultrafine-grained (UFG) states of billets made from different metals and alloys to be formed. These states are characterized by attractive properties and have high potential for industrial applications. Extraordinary mechanical properties of bulk nanostructured materials are of special interest. In [1] it was demonstrated that materials subjected to SPD can have a very high strength combined with sufficient ductility, high fatigue strength, and low-temperature or high-strain-rate super-ductility. These bulk nanostructured materials manufactured by the SPD are characterized by extremely small grain sizes and high density of crystal structure defects on the grain boundaries. Moreover, they are highly nonequilibrium [1–3]. At the same time, wide industrial application of the UFG metallic materials calls for a study of the influence of traditional methods of deformation processing on the evolution of their microstructure, crystallographic texture, and mechanical properties.

Flat rolling is one of the traditional processing techniques widely used to obtain industrial products. The rolled material is conventionally characterized by the fine-grained structure and developed crystallographic texture. The x-ray diffraction (XRD) analysis allows coherent scattering domain (CSD) sizes, elastic crystal lattice microdistortions, dislocation density, activity of slip and twinning systems, etc. to be estimated. It can also be used successfully to monitor microstructural changes and to establish mechanisms leading to these changes [4].

The results of XRD analysis of the microstructure of titanium and its alloys subjected to ECAP, HPT, and MAF with subsequent rolling have been presented in a number of papers (for example, see [5–9]). In particular, it has been found that MAF with 4 cycles of the VT6 alloy in the temperature interval 750–650 °C does not lead to substantial  $\alpha \rightarrow \beta$  transformation [7]. The microstructure is characterized by high density of incorporated defects, CSD size reduced 3 folds, and doubled elastic microdistortions of the crystal lattice compared to the initial state [7].

The microstructure of the VT6 alloy subjected to MAF is characterized by the  $\alpha$ - and  $\beta$ -phase grains with an average size of 0.4  $\mu\text{m}$ , high level of long-range stresses, and microdistortions of the crystal lattice, as evidenced by

---

<sup>1</sup>Ufa State Aviation Technical University, Ufa, Russia, e-mail: svil@mail.rb.ru; iva@mail.rb.ru; <sup>2</sup>Institute for Metals Superplasticity Problems of the Russian Academy of Sciences, Ufa, Russia, e-mail: vdan@imsp.ru; vladimirp@imsp.ru. Translated from *Izvestiya Vysshikh Uchebnykh Zavedenii, Fizika*, No. 6, pp. 30–33, June, 2015. Original article submitted March 6, 2015.

the non-uniform diffraction contrast and high dislocation density on electron microscopic images of the structure [8]. At present investigations of the influence of flat rolling on the microstructure and crystallographic texture of titanium alloys with UFG structure are far from being completed. For example, the effect of cold rolling of technically pure titanium with UFG structure formed by the ECAP was studied in [9]. The full-profile analysis of XRD patterns demonstrated that the mean CSD size after rolling of UFG-titanium with 73% reduction was 39 nm, the volume fraction of dislocations  $\langle a \rangle$  was 66%, that of  $\langle c \rangle$  was 33%, and that of  $\langle a + c \rangle$  was 1%, respectively. At the same time, a comprehensive analysis of the microstructure evolution during rolling of the UFG titanium alloy has not yet been performed.

The purpose of the present paper is to study the influence of flat rolling on the structure of the VT6 titanium alloy using XRD analysis of both initial and UFG states after isothermal multiaxial forging.

## MATERIAL, EXPERIMENTAL PROCEDURE, AND MODELING TECHNIQUE

Billets of the VT6 titanium alloy (volume fractions of the elements, in %: Fe  $\leq$  0.3, C  $\leq$  0.1, Si  $\leq$  0.15, V  $\leq$  5.3, N  $\leq$  0.05, Ti  $\leq$  91.2, Al  $\leq$  6.8, Zr  $\leq$  0.3, O  $\leq$  0.2, and H  $\leq$  0.015) with average grain size of 10  $\mu\text{m}$  annealed at 700°C for 5 h were chosen as initial material. They were shaped as rectangular parallelepipeds 250 mm long with the square base having a side of 11 mm. The billets were subjected to MAF at 650°C with 6 forging cycles. Then they were subjected to cross rolling in a LIS 6/200 rolling mill with 75 and 95% reduction at a temperature of 550°C. After three passes, the specimen was rotated through 90° and then was subjected to three more passes. In this case, the thickness of the billet was reduced from 12 to 0.8 mm. The XRD analysis was performed with a Rigaku Ultima IV diffractometer using  $\text{CuK}\alpha_1$  radiation ( $\lambda = 0.154060$  nm) at a voltage of 45 kV and a current of 40 mA. The x-ray peaks were registered with a step of 0.01° and a counting time of 2 s. The CSD size  $D$  and the elastic lattice microdistortions  $\langle \varepsilon^2 \rangle^{1/2}$  were quantitatively estimated using the software package *PDXL* (www.rigaku.com).

## RESULTS AND DISCUSSION

The XRD pattern of the VT6 alloy specimen in the initial state (Fig. 1a) is characterized by a number of main x-ray peaks with the  $(10\bar{1}0)$ ,  $(0002)$ ,  $(10\bar{1}1)$ ,  $(10\bar{1}2)$ ,  $(11\bar{2}0)$ ,  $(10\bar{1}3)$ ,  $(20\bar{2}0)$ ,  $(11\bar{2}2)$ , and  $(20\bar{2}1)$  Miller indices corresponding to pure  $\alpha$ -Ti (HCP lattice). In addition, the XRD pattern contains weak  $(110)$ ,  $(200)$ ,  $(211)$ , and  $(220)$  peaks characteristic for the Ti  $\beta$ -phase (BCC lattice). The quantitative phase analysis demonstrated that the volume fraction of the  $\beta$ -phase in the alloy was 14.6%.

After MAF that caused the formation of the UFG state, the volume fraction of the  $\beta$ -phase decreased down to 12.4%, and that of the  $\alpha$ -phase increased up to 87.6% in comparison with the initial state. Investigations of the billets in the rolled state demonstrated further decrease of the volume fraction of the  $\beta$ -phase and increase of the  $\alpha$ -phase (Table 1).

Not only after MAF, but also after subsequent rolling the lattice parameter  $a$  and hence, the volume of the unit  $\alpha$ -phase cell tend to decrease. This decrease may be due to segregation of impurity atoms of chemical elements, such as Al and V, at the grain boundaries or inside of grains because of the decrease of the  $\beta$ -phase fraction since, as is well known, exactly these impurity atoms ensured the stability of the  $\beta$ -phase at intermediate temperatures. The radii of the Ti, Al, and V atoms were equal to 147, 143, and 134 pm, respectively. After the  $\beta$ -phase decay, Al and V atoms were dissolved in the  $\alpha$ -phase lattice and became substitutional impurities. Since the radii of Al and V atoms are smaller than the radius of the Ti atoms, this process should lead to a decrease in the lattice parameter which was observed experimentally.

The XRD patterns of the alloy in the UFG state (Fig. 1b) and in the UFG state with additional rolling (Fig. 1c and d) have a number of peaks characteristic for the alloy in the initial state. However, many of them were essentially broadened (Table 1), whereas the peaks in the initial state were narrow, and their intensity was quite high. For example, in the initial state the broadening of the  $(0002)$  peak in the range of small angles and the  $(10\bar{1}3)$  peak in the range of great angles  $2\theta$  was 0.102 and 0.139°, respectively. In the UFG state after MAF, the broadening increased to 0.202 and

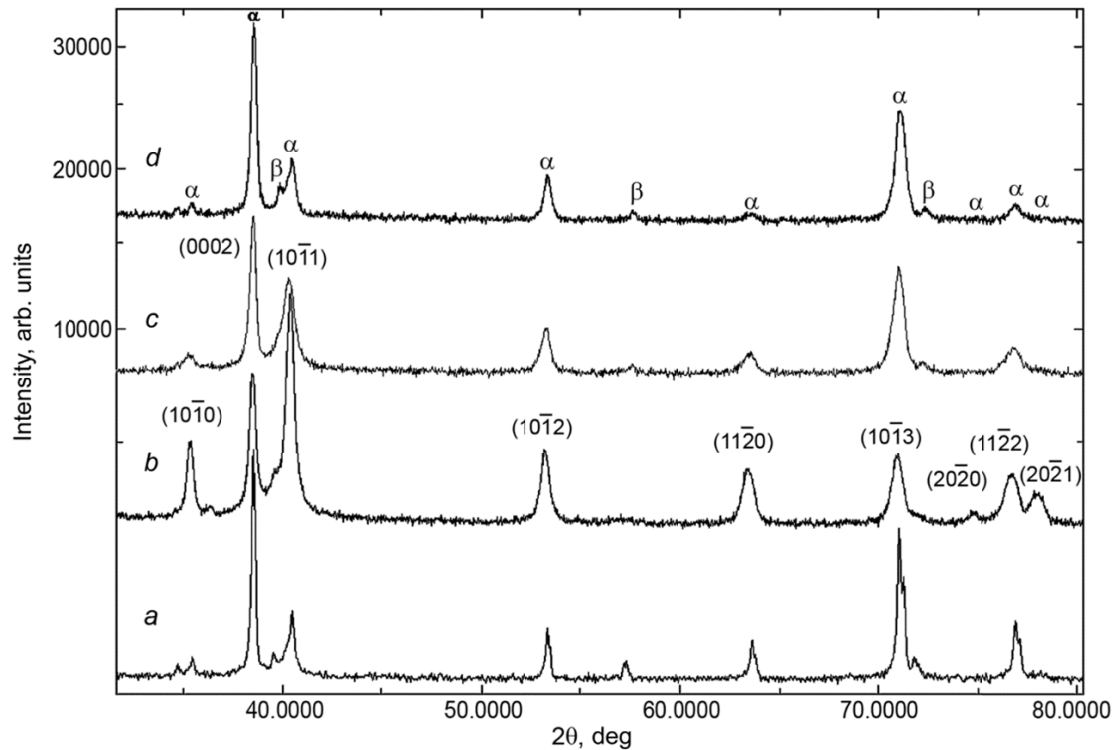


Fig. 1. X-ray diffraction patterns of the VT6 titanium alloy in different structural states. Here *a* is the initial annealed state, *b* is the UFG state, *c* is the UFG state with subsequent rolling reduction of 75%, and *d* is the UFG state with subsequent rolling reduction of 95%.

0.396°, respectively. At the same time, the total peak intensities were redistributed as a result of MAF. This was especially well pronounced for the  $(10\bar{1}0)$ ,  $(0002)$ ,  $(10\bar{1}1)$ ,  $(10\bar{1}2)$ ,  $(21\bar{3}1)$ , and  $(20\bar{2}1)$  peaks. These peaks characterize the specific fraction of *prismatic*, *basic*, and *pyramidal* crystallographic planes of the HCP lattice in x-ray scattering of the specimen. The last is the evidence of the evolution of the crystallographic texture as a result of MAF.

To analyze the peak profiles on XRD, the pseudo-Voigt function comprising the Gauss and Lorentz components was applied. The Gauss component characterizes sharper maxima, and broadened maxima correspond to the Lorentz component. Qualitative comparison of the profiles of different peaks for the initial and UFG states demonstrated some differences in the relative fraction of the Lorentz component in the profiles of individual peaks. Its contribution to the UFG state was 85–95%. We note that the peaks in the initial state were narrow, and their intensity was quite high.

The revealed changes in the contributions of the Gauss and Lorentz components and peak broadening were caused by MAF that led to changes in the CSD size distribution and in the character of the defect structure depending on the texture component to which grains belong. Thus, MAF led to essential changes in the microstructure of the initial coarse-grained state.

A comparative analysis of the microstructure characteristics recorded by the XRD method showed that the volume fractions of  $\alpha$ - and  $\beta$ -phases in the UFG state, the lattice parameters, the sizes of coherent scattering domains, the level of elastic microdistortions of the crystal lattice, and the dislocation density in the  $\alpha$ -phase essentially differed from those in the initial state (Table 1). In particular, the CSD size in the  $\alpha$ -phase of the VT6 titanium alloy decreased after MAF by approximately 3.8 times and was  $(29 \pm 4)$  nm. This value did not contradict the results presented in [9] for UFG titanium (grade 2) manufactured by the ECAP. Rolling of the UFG state led to a decrease in the CSD size down to  $(24 \pm 3)$  and  $(18 \pm 3)$  nm with 75 and 95% reduction, respectively.

TABLE 1. Microstructure Parameters of the VT6 Alloy Billets

State	Volume fraction, %		$a$ and $c$ , Å	Broadening, deg		CSD, nm	$\langle \epsilon^2 \rangle^{1/2}$ , %	$\rho$ , $10^{15} \text{ m}^{-2}$
	$\alpha$ -phase	$\beta$ -phase	$\alpha$ -phase	(0002)	(10 $\bar{1}$ 3)	$\alpha$ -phase	$\alpha$ -phase	$\alpha$ -phase
Initial	85.4(8)	14.6(4)	2.9364(5) 4.6743(7)	0.102(5)	0.139(4)	112(14)	0.12(2)	0.8(2)
MAF (UFG)	87.6(7)	12.4(4)	2.9273(4) 4.6659(8)	0.202(3)	0.396(7)	29(5)	0.27(4)	8.1(4)
MAF (UFG) + 75% rolling	90.8(4)	9.2(3)	2.9244(4) 4.6654(8)	0.237(5)	0.457(8)	24(4)	0.31(4)	8.7(8)
MAF (UFG) + 95% rolling	91.3(5)	8.7(4)	2.9190(5) 4.6641(9)	0.292(4)	0.516(9)	18(3)	0.36(5)	11.8(7)

The level of elastic microdistortions of the crystal lattice in the UFG state exceeded the analogous value corresponding to the initial state by a factor of 2.25 and by a factor of 3 after a 95% rolling reduction. In addition, the dislocation density in the UFG state was by an order of magnitude greater than in the initial state, and after rolling with 75 and 95% reduction, it reached  $8.7 \cdot 10^{15}$  and  $11.8 \cdot 10^{15} \text{ m}^{-2}$ , respectively. The dislocation density (Table 1) was slightly higher than the dislocation density of pure titanium after eight ECAP passes and subsequent cold rolling ( $\rho \sim 3 \cdot 10^{15} \text{ m}^{-2}$ ) [9]. These differences, obviously, were related with the purity of the materials being compared and the strain degree and temperature.

## CONCLUSIONS

The XRD analysis has shown that the volume fraction of the  $\beta$ -phase decreased by more than 1.5 times after MAF and subsequent rolling with a 95% reduction. Wherein, the alloying elements were dissolved in the  $\alpha$ -phase, which led to the decrease of its lattice parameter. At the same time, additional rolling led to the broadening of the XRD peaks due to the increase of elastic microdistortions of the crystal lattice and the dislocation density and the decrease of the CSD size.

This work was supported in part by Russian Foundation for Basic Research (grant No. 14-08-97052 r\_povolzh'e\_a).

## REFERENCES

1. R. Z. Valiev, R. K. Islamgaliev, and I. V. Alexandrov, *Prog. Mater. Sci.*, No. 45, 103–189 (2000).
2. R. Z. Valiev and T. G. Langdon, *Prog. Mater. Sci.*, No. 51, 881–981 (2006).
3. R. Z. Valiev and I. V. Alexandrov, *Bulk Nanostructured Metallic Materials* [in Russian], Moscow, Akademkniga (2007).
4. S. S. Gorelik, L. N. Rastorguev, and Yu. A. Skakov, *X-Ray and Electron-Optical Analysis* [in Russian], Moscow Institute of Steel and Alloys Publishing House, Moscow (2002).
5. I. Kim, J. Kim, D. H. Shin, *et al.*, *Scripta Mater.*, No. 48, 813–817 (2003).
6. E. Schafler, M. Zehetbauer, and T. Ungar, *Mater. Sci. Eng.*, No. A319–321, 220–223 (2001).
7. R. G. Zariпова, V. A. Shundalov, A. V. Sharafutdinov, *et al.*, *Vestn. Ufimsk. Gosud. Aviats. Tekh. Univ.*, **16**, No. 7(52), 17–24 (2012).
8. S. Zherebtsov, G. Salishchev, R. Galeev, and K. Maekawa, *Mater. Trans.*, **46**, No. 9, 2020–2025 (2005).
9. J. Gubicza, I. C. Dragomir, G. Ribárik, *et al.*, *Z. Metallkunde*, No. 94, 1185–1196 (2003).